



# Improved prediction of wet snow

Emilie C. Iversen<sup>1,2</sup>, Gregory Thompson<sup>3</sup>, Bjørn Egil Nygaard<sup>1</sup>, Matteo Lacavalla<sup>4</sup>

<sup>1</sup> Kjeller Vindteknikk AS, Norway

<sup>2</sup> University of Oslo, Norway

<sup>3</sup> National Centre for Atmospheric Research, CO, USA

<sup>4</sup> RSE SpA, Research on the Energy System, Milan, Italy

emilie.iversen@vindteknikk.no, gthompsn@ucar.edu, bjorn.nygaard@vindteknikk.no, matteo.lacavalla@rse-web.it

**Abstract—** This paper presents the first results from research on improving prediction of snow falling through the melting layer in a NWP model microphysics scheme, which will contribute to improve predictions of wet snow icing. Modifications to the scheme are related to location of melting level and the fall speed of melting snowflakes, where two different methods are presented. Continued research will utilize observations from disdrometer measurements to validate the changes performed to the microphysics scheme.

**Keywords—** Wet snow, melting layer, NWP modelling, WRF, Thompson microphysics

## I. INTRODUCTION

Snow falling into the melting layer will eventually consist of a fraction of melted water and become sticky. The sticky snow can be problematic for structures in the way that it can adhere to objects and create an ice sleeve [1]. Wet snow icing has shown to be particularly problematic for overhead transmission lines, with events causing tower collapses and power outages in all continents of the northern hemisphere, as well as in New Zealand, South Africa and Argentina [2]. Obtaining precise predictions of wet snow and mixed precipitation from numerical weather prediction models is important to prevent costly damages of infrastructure, as well as for human safety. It is hence important that the relevant models incorporate a microphysical scheme with a good representation of precipitation in the melting layer, without being too computationally expensive to run in real-time. Relatively little attention has been given to development and testing of bulk microphysical schemes in relation to winter type precipitation prediction given the importance [3]. The Thompson microphysics scheme has been developed and tested for forecasting winter precipitation as part of the WRF model (Weather Research and Forecast model), and is viewed to be perhaps the best real-time, bulk scheme for icing forecasting due to the specific development towards in-cloud aircraft icing [4]. Less attention has though been devoted to melting snow and wet snow icing, which most often occur close to the ground. This paper presents preliminary results from research on improving the Thompson microphysics scheme with respect to the representation of melting snow. In section II particularly interesting observations of melting snow are presented, serving as a base for modifying the scheme. In section III parts of the current Thompson scheme relevant for the behavior of melting snow is described, as well as changes performed to improve this behavior through this research. Section IV describes the data used and section V presents the results. A discussion is carried out in section VI.

## II. OBSERVATIONS OF MELTING SNOW

Laboratory experiments by [5] (hereafter Mitra90) using a vertical wind tunnel provides a detailed insight into the behavior of snow falling through the melting layer. Their observations showed that during the initial stage of melting of the snowflakes, fall velocities varied very little and began to increase rapidly after about 70% of the original mass was melted (Fig. 1), which agrees well with disdrometer measurements studied by [6]. From this it seems that fall velocity of wet snow is a non-linear function of its melted fraction, and is not simply explained by particle size. They also found a close to linear relationship between the fraction of particle mass melted and the vertical distance travelled to obtain this melted fraction (melt distance). If the relative humidity (RH) was less than 100% the particles travelled some distance before melting began due to evaporative cooling, and the melt distance was increased.

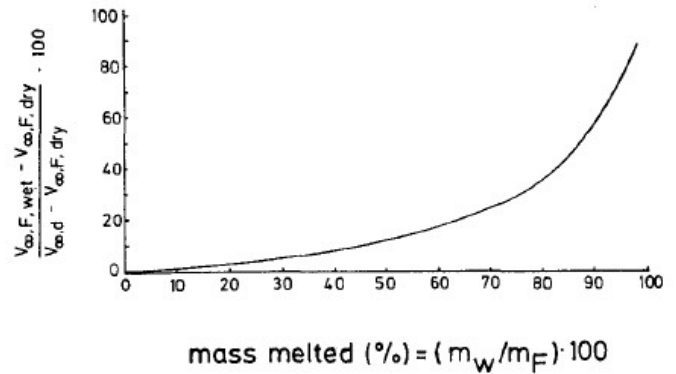


Fig. 1 Variation of the fractional fall velocity of melting snow flakes as a function of the fractional mass melted for 10 and 5 mm diameter flakes present in wind tunnel results by Mitra90.  $V_F$ : fall velocity of melting flakes,  $V_{\infty,d}$ : terminal fall velocity of drops into which the flake melted,  $V_{\infty,F}$ : terminal fall velocity of dry snow flake,  $m_w$ : mass of melt water in flake,  $m_F$ : mass of dry flake, (for about 45 snowflakes).

The importance of RH on the melting level and precipitation phase has been stressed by many authors. In subsaturated conditions, sensible and latent heat exchange between the air and the falling precipitation particle determine its temperature and ultimately its phase [7]. The wet bulb temperature ( $T_w$ ) contains air temperature ( $T_a$ ), humidity and pressure information, and precipitation particle surfaces have a temperature closer to  $T_w$  than  $T_a$  [8, 9]. Therefore  $T_w > 0^\circ\text{C}$  is a better criterion for melting [10].

### III. THE MICROPHYSICS SCHEME

In most widely used bulk microphysics schemes, including the Thompson scheme, there is no prognostic variable explicitly representing the “melting particle” species. As snow falls across the melting level, parts of its mass is transferred over to the rain category, according to a heat balance calculation. The associated size distributions also change accordingly, gradually widening the distribution of rain, introducing larger drops, while shrinking the distribution of snow, leaving the smallest snowflakes, as snow is melting. As the fall speed of snow starts to change and deviate from that of dry snow when entering the melting layer, an explicit expression for its fall speed is needed, based on the properties of the dry snow and rain species.

#### A. Relevant details of the microphysics scheme

The hydrometeor fall velocity relations in the scheme are combinations of power-laws and exponentials following [11]:

$$v(D) = \left(\frac{\rho_0}{\rho}\right)^{\frac{1}{2}} \alpha D^\beta e^{-fD} \quad (1)$$

The values of the constants can be found in Table A1 in [4]. To explicitly express the fall speed of melting snow, melting is identified where  $T_a > 0^\circ\text{C}$ . In the code preceding WRF version 3.8 this fall speed was simply equaled to the maximum of the fall speed of rain and dry snow at that level (hereafter Old Method). In the code following WRF version 3.8 an expression was implemented where the fall speed is an inverse function of temperature:

$$V_m = V_s \frac{V_r - V_s}{T - T_0} \quad (2)$$

where  $V_m$ ,  $V_s$  and  $V_r$  are the terminal velocities of melting snow, dry snow and rain, respectively, and  $T - T_0$  represents the number of degrees above  $0^\circ\text{C}$   $T_a$ . Given this expression the fall speed will decrease as the temperature increase above  $0^\circ\text{C}$ , indicating a decrease in fall speed with melting degree, which is opposite to what Mitra90 found. As this most likely is a bug in the code, results using this version of the code will not be shown in this study.

The scheme also introduces a boosting factor applied to the fall speed of dry snow, which is given as a function of the degree of riming of the snowflakes. For the sake of highlighting the results purely connected to the fall speed of melting snowflakes, this boosting factor is removed in the code used in this study.

#### B. Changes performed to the scheme

Given the emphasis on the dependence of melting and precipitation type on RH and the use of  $T_w$  in the literature, melting is defined where  $T_w > 0^\circ\text{C}$ . Given the findings by Mitra90 the fall speed of melting snow should be expressed as a function of its melted fraction. To maintain the current computational cost of running the scheme, the introduction of an additional prognostic variable such as the melted fraction is to be avoided. Though, we can utilize the ratio of rain to snow present in an air volume within the melting layer as a liquid ratio (LR) for that volume [12]:

$$LR = Q_{RAIN} / (Q_{RAIN} + Q_{SNOW}) \quad (3)$$

where  $Q_{RAIN}$  and  $Q_{SNOW}$  are the mixing ratios of rain and snow in the model. This though assumes that all rain particles present at all vertical levels within the melting layer are generated from snow melting at that same level [13]. This could introduce errors in some cases because 1) rain could be produced from convection within the melting layer, and 2) rain falls faster than snow, so at any level most of the rain has originated from a level above. Anyhow, the use of LR can give a physically based approximation of the average liquid fraction in the melting layer, without the addition of an extra prognostic variable.

Using the LR, the expression for fall speed of melting snow is changed in two different ways, resulting in two different methods:

1) *Method 1*: A simple linear function weighting the fall speed of dry snow and rain with their respective fraction was used to linearly increase the fall speed of melting snow as the LR increase:

$$V_m = (1 - LR)V_s + LRV_r \quad (4)$$

2) *Method 2*: In their bulk parameterization scheme, [14] expressed fall speed of melting snow as a function of liquid fraction, where the liquid fraction is the calculated melted mass over total mass of the snowflakes. The expression was made to fit perfectly with the relationship found by Mitra90:

$$V_m(f) \approx \frac{1}{g(f)} V_r \quad (5)$$

$$\text{where } g(f) \approx \frac{a}{\alpha} - c_g f - c_g f^2, \quad (6)$$

$f$  is the liquid fraction,  $V_r$  is the terminal velocity of the rain in which the snow melted into,  $a/\alpha=4.6$  and  $c_g=0.5$ . Here we substitute  $f$  with LR. The expression is derived from the fall velocity relations for dry snow and rain. In [14] these relations are simple power-law functions dependent on the melted diameter, given by [15] and [16]. The fall velocity relations in the Thompson scheme are combinations of power-laws and exponentials shown in (1). Due to this difference, the expression given in (5) and (6) is here modified to obtain consistent fall speeds when  $LR = 0$  (dry snow) and  $LR = 1$  (rain), maintaining the relationship of Mitra90.

### IV. DATA

Observational data from the Wet snow Icing Laboratory Detection (WILD) realized and managed by RSE in the southern Italian Alps have been made available, including measurements of ice accumulation on erected test spans and disdrometer measurements [17]. Numerous events of wet snow icing have been registered at the site. A WRF simulation with a domain covering the Italian Alps was set up to test how the microphysics scheme, including the two different methods introduced, was able to replicate these conditions. The simulation is run with two nested domains, with 15 km and 3 km horizontal resolution, 72 vertical levels, and ERA-Interim boundary data. The domain, the location of the WILD station and a line representing a vertical cross section (for which results are to be presented in the Results

section) is shown in Fig 2. An event is picked out to simulate; 24-26 December 2013, when a low pressure system was moving from north-western Europe over the Alps causing heavy snowfall, and 5 kg/m of wet snow ice accretion on the test span. The disdrometer measurements during this event reveal a bimodal distribution typical of melting snow and mixed precipitation (Fig. 3) (see [6]). It should be noted that the objective of this paper is not to present direct comparisons with the observations, but to highlight the effect of the changes performed to the scheme.

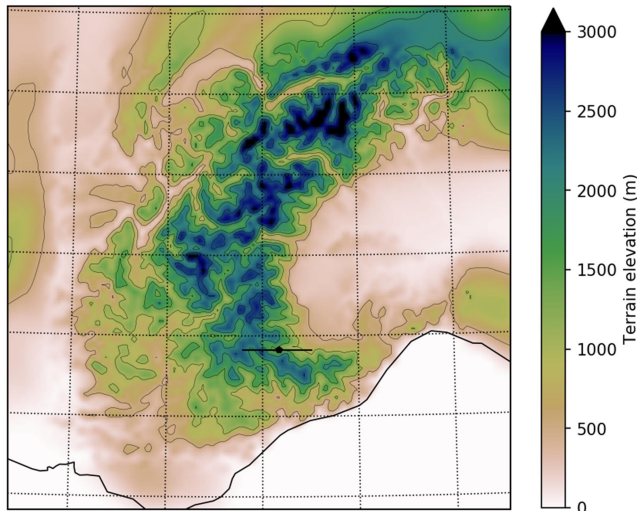


Fig. 2 Inner model domain with a 3 km horizontal resolution, showing terrain height (colors), the location of the WILD station (black dot), and the vertical cross section (black line).

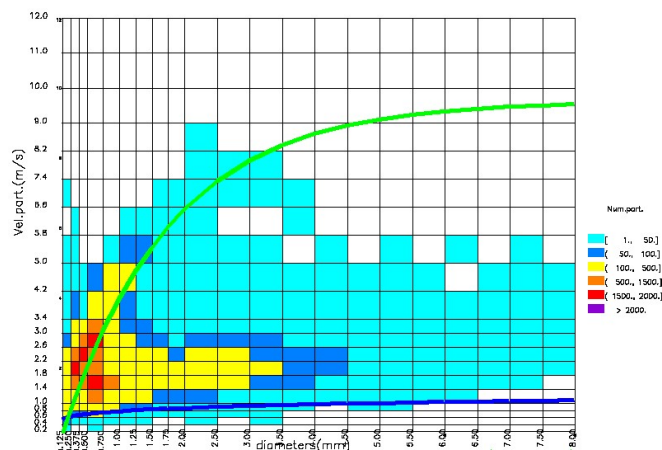


Fig. 3 Disdrometer measurement of precipitation diameter versus fall velocity from the WILD station during the event. The green line shows a typical distribution for rain and the blue line for dry snow. The color scale represents the total number of particles integrated over the hour.

## V. RESULTS

Fig. 4 (top panels) show fall velocities of melting snow (for instances when  $T_a > 0^\circ\text{C}$  for the Old method, and  $T_w > 0^\circ\text{C}$  for Method1 and Method2) versus LR. It is evident that the Old method displays no relationship with LR; Method1 a linear relationship; and Method2 a non-linear relationship in

agreement with Mitra90. The color scale reveal the effect that the mass weighted mean diameter (MWMD) of the snowflakes shrink as melting is progressing and LR is increasing, due to the transfer of mass from the snow to the rain category like mentioned.

Fall velocities of rain, dry snow and melting snow are plotted versus MWMD in Fig. 4 (middle panels). Fall velocities of melting snow are increasing from typical fall velocities of dry snow towards typical fall velocities of rain as melting progresses, similar to what can be seen in the disdrometer measurements (Fig. 3). Again it is evident that there is a better relationship between fall velocity and LR for the two new methods compared to the Old. This figure confirms how Method2 gives fall velocities for melting snow similar to those of dry snow for  $LR < 0.4$  and gives a rapid increase towards typical rain velocities for  $LR > 0.7$ , giving a more bimodal distribution similar to the disdrometer measurements. Method 1 gives a more steady increase due to the linear relationship. For almost completely melted snowflakes, MWMD is not corresponding to those of rain of the same fall speeds using either of the methods. This is again due to the shrinking of MWMD of the snow size distribution with melting. In reality, the smallest snowflakes will melt first, implying a shift towards larger MWMDs.

A vertical cross section is made through the valley where the WILD station is located (indicated in Fig. 2) to explore the vertical evolution of snow fall speed through the melting layer (Fig. 4, bottom panels). Using the Old method, it can be seen that melting is initiated when the  $0^\circ\text{C}$   $T_a$  isotherm is crossed. Melting level is determined at  $T_w = 0^\circ\text{C}$  using Method1 and Method2, and it can be seen that snow falls a longer vertical distance below melting level before fall speeds are starting to increase using Method2 than Method1. Approaching the bottom of the melting layer over the lower terrain (about 1100 m) to the east in the valley, where  $T_w > 1^\circ\text{C}$ , Method2 produces fall speeds that are 1-2 m/s higher than those produced by Method1. At the location of the measuring site (about 1300 m in the WRF terrain) where  $0 < T_w < 1^\circ\text{C}$ , Method 1 produces fall speeds that are 0.5-1.5 m/s higher than those produced by Method2. These differences are produced by the linear versus the non-linear relationship of fall speed and degree of melting between Method1 and Method2, respectively.

## VI. DISCUSSION

The representation of partially-melted snow in a numerical model is difficult. Nearly all microphysics schemes assume that melt water immediately “sheds” directly into the rain category leaving behind only the remaining mass of snow as if it was a dry and smaller snowflake. Observations have shown that the melt water is contained within the crystal, so that a “ragged” surface of a crystal is maintained for some time, up until the water overtakes the crystal to form a water droplet [18, 19, 20, 5]. According to [5] the “transformation” from a snowflake structure to a raindrop structure occur approaching 70% liquid fraction. The implementation of the dependence of melting snow fall speed on liquid ratio in this study does take this into account in terms of fall speed characteristics, but not in terms of mass, and hence size of the snow particles. The assumption of melted water shed to the rain category produces snow particle sizes that are

smaller than the actual partly-melted snow, which further affects the evaporation rates. When developing microphysics schemes with specific focus on melting precipitation, [14] and [3] introduced a “cutoff” diameter for the snow size distribution representing the minimum diameter of snowflakes not completely melted, obtained through a relationship with the diagnosed snowflake melted

fraction. This minimum diameter determines when part of the snow mass is transferred to the rain category. The computational cost of adding new variables to the Thompson scheme may not be worthwhile considering how rapidly snow generally melts and how far spread are the model levels in the vertical.

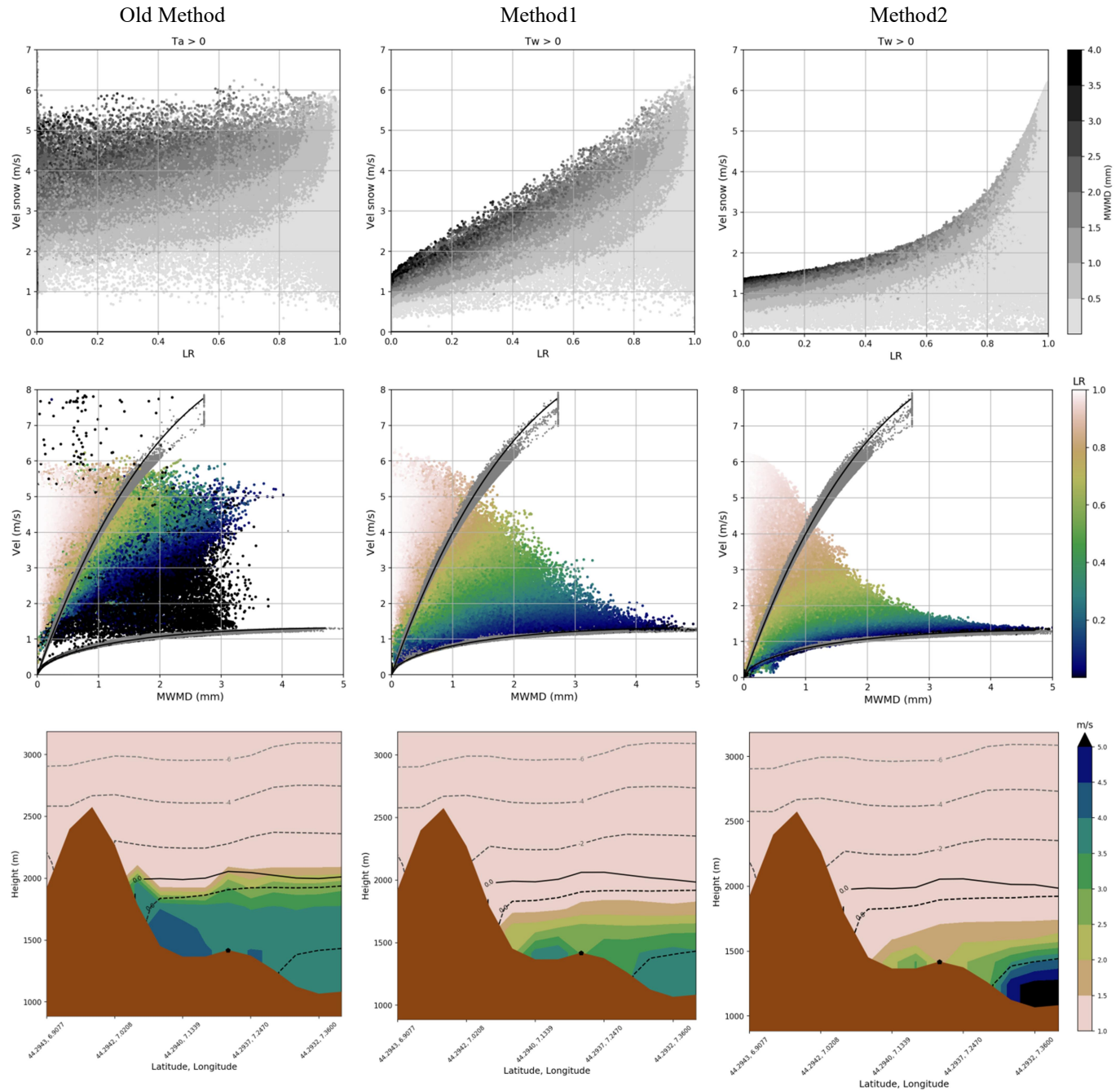


Fig. 4 Comparison of the Old Method (leftmost panels), Method1 (middle panels) and Method2 (rightmost panels) from a WRF simulation (shown in Fig. 2) for the event 24-25 December 2013 at WILD station in the southern Italian Alps. Top: Liquid ratio (LR) versus velocity of melting snow at model level 1 (ML1) for the whole event, the color scale indicates MWMD. Middle: MWMD versus velocity of all precipitation at ML1 for the whole event. The grey points indicate rain (lowermost) and dry snow (uppermost), and the black line through them are the direct velocity relations from [11]. The rest of the dots plotted with a color scale is melting snow, where the scale indicate LR. Bottom: Instantaneous vertical cross sections (indicated in Fig. 2) of the melting layer showing velocity of snow with the color scale, wet bulb temperature isotherms with dashed lines, and the 0°C air temperature isotherm with a solid black line.



Ultimately, what determines precipitation phase in the scheme are the heat balance equations and associated transfer of mass from the snow to the rain category, the definition of melting level, and the expressions for fall speed, all together determining the rain to snow ratio. The improved definition of melting level and expressions for melting snow fall speed presented here will contribute to improve the prediction of precipitation phase, and the latter could be of large importance due to the overall mass flux and precipitation rate along with properly representing the overall depth of melting particles. Further research will utilize ground observations of wet snow events for direct comparison with model output to determine if the performed changes produce improvements and what additional improvements might be needed.

#### ACKNOWLEDGMENT

This work is financed by Statnett, the Norwegian TSO, through the research project ICEBOX. The author would like to thank RSE and Matteo Lacavalla for sharing observational data from the WILD measuring site in Italy.

#### REFERENCES

- [1] L. Makkonen, "Estimation of wet snow accretion on structures," *Cold Region Sci. Technol.*, 17, pp. 83-88, 1989.
- [2] B. Nygaard, S. M. Fikke and L. Makkonen, "State of the art report on designing transmission lines for wet snow accumulation," CEATI, 2017.
- [3] J. M. Thériault and R. E. Stewart, "A Parameterization of the Microphysical Processes Forming Many Types of Winter Precipitation," *J. Atmos. Sci.*, 67, pp. 1492-1508, 2010.
- [4] G. Thompson, P. R. Field, R. M. Rasmussen and W. D. Hall, "Explicit Forecasts of Winter Precipitation Using an Improved Bulk Microphysics Scheme. Part II: Implementation of a New Snow Parameterization," *Mon. Wea. Rev.*, 136, pp. 5095-5115, 2008.
- [5] S. K. Mitra, O. Vohl, M. Ahr and H. R. Pruppacher, "A wind tunnel and theoretical study of the melting behavior of atmospheric ice particles. IV: Experiment and theory for snow flakes," *J. Atmos. Sci.*, 47, pp. 584-591, 1990.
- [6] S. E. Yuter, D. E. Kingsmill, L. B. Nance and M. Löffler-Mang, "Observations of Precipitation Size and Fall Speed Characteristics within Coexisting," *J. applied meteorology and climatology*, 45, pp. 1450-1464, 2006.
- [7] R. E. Stewart, "Precipitation Types in the Transition Region of Winter Storms," *Bull. Amer. Meteor. Soc.*, 73, pp. 287-296, 1992.
- [8] P. Harder and J. Pomeroy, "Estimating precipitation phase using a psychrometric energy balance method," *Hydrol. Process.*, 27, pp. 1901-1914, 2013.
- [9] B. Ding, K. Yang, J. Qin, L. Wang, Y. Chen and X. He, "The dependence of precipitation types on surface elevation and meteorological conditions and its parameterization," *J. Hydrol.*, 513, pp. 154-163, 2014.
- [10] L. Makkonen, "Estimation of wet snow accretion on structures," *Cold Reg. Sci. Tech.*, 17, pp. 83-88, 1989.
- [11] B. S. Ferrier, "A double-moment multiple-phase four-class bulk ice scheme. Part I: Description," *J. Atmos. Sci.*, 51, pp. 249-280, 1994.
- [12] B. E. K. Nygaard, H. Ágústsson and K. Somfalvi-Tóth, "Snow Accretion on Power Lines: Improvements to Previous Methods Using 50 Years of Observations," *J. Appl. Met. & Clim.*, Vol. 52, pp. 2189-2203, 2013.
- [13] J. A. Milbrandt, A. Glazer and D. Jacob, "Predicting the Snow-to-Liquid Ratio of Surface Precipitation Using a Bulk Microphysics Scheme," *Mon. Wea. Rev.*, 140, pp. 2461-2476, 2012.
- [14] W. Szyrmer and I. Zawadzki, "Modeling of the Melting Layer. Part I: Dynamics and Microphysics," *J. Atmos. Sci.*, 56, p. 3573-3592, 1999.
- [15] M. Langleben, "The terminal velocity of snowflakes," *Quart. J. Roy. Meteor. Soc.*, pp. 174-181, 1954.
- [16] K. L. S. Gunn and G. D. Kinzer, "The terminal velocity of fall for water droplets in air," *J. Meteor.*, 6, pp. 243-248, 1949.
- [17] M. Lacavalla, P. Marcacci and A. Freddo, "Wet snow activity research in Italy," *Proc. IWAIIS*, 2015.
- [18] C. A. Knight, "Observations of the morphology of melting snow," *J. Atmos. Sci.*, 36, pp. 1123-1130, 1979.
- [19] T. Matsuo and Y. Sasyo, "Empirical formula for the melting rates of snow flakes," *J. Meteor. Soc. Japan*, 59, pp. 1-8, 1981a.
- [20] Y. Fujioshi, "Melting snow flakes," *J. Atmos. Sci.*, 43, pp. 307-311, 1986.